Research Article

A 3-Dimensional Multiband Antenna for Vehicular 5G Sub-6 GHz/ GNSS/V2X Applications

Ahmad S. Ibrahim ⓘ**, Ahmad M. Yacoub** ⓘ**, and Daniel N. Aloi** ⓘ

Electrical and Computer Engineering Department, Oakland University, Rochester Hills, MI 48309, USA

Correspondence should be addressed to Ahmad S. Ibrahim; asalihibrahim@oakland.edu

A compact multiband monopole antenna is proposed for vehicular roof top shark-fin applications. The proposed multiband antenna covers 5G sub-6 GHz and LTE bands starting at 617 MHz to 5000 MHz and the higher GNSS band from 1559 to 1606 MHz as well as the V2X band at 5900 MHz. The presented antenna is a three-dimensional monopole antenna with two branches to cover the required bands with compact size to fit inside a roof top shark-fin. The long antenna branch covers the lower cellular frequency band from 617 to 960 MHz, while the short branch covers the higher frequency band from 1559 to 6000 MHz. The presented antenna is mounted on a double-sided FR4 PCB and is feeded through a short cable. The proposed antenna covers multiple frequency bands with compact size (H x L x W) of $58 \times 37 \times 17$ mm^3. The antenna is simulated and optimized, and then, a prototype is fabricated, and its radiation characteristics are measured when mounted on one-meter ground plane and on a vehicle's roof. The maximum measured linear average gain is 3 dBi at 1900 MHz, and the maximum measured efficiency is 88% at 787 MHz. The active GNSS antenna gain is measured using an LNA with good isolation. A good agreement is achieved between the simulated and measured results when compared in terms of voltage standing wave ratio (VSWR), radiation patterns, linear average gain (LAG), and antenna efficiency.

1. Introduction

Vehicular communication research and development has spiked recently due to the introduction of autonomous driving and intelligent vehicles, which requires many communication systems and protocols to be implemented [1]. To improve safety and efficiency in vehicles and the whole transportation system, vehicle-to-everything (V2X) is introduced, which mainly includes vehicle-to-vehicle (V2V), vehicle-to-pedestrian (V2P), vehicle-to-infrastructure (V2I), and vehicle-to-network (V2N). By exchanging messages between vehicles, infrastructure, and pedestrians, V2X can support many use cases such as forward collision warning, parking search, and optimizing a vehicle's traffic [2]. Another revolutionary technology for vehicle autonomy is the 5G cellular communications, which provides a reliable and low latency communications as well as high data rates. 5G wireless network provides an essential role by providing a

reliable and fast communication between vehicles and other objects which means it can be integrated with V2X and this integration called later as cellular V2X (C–V2X). Global Navigation Satellite System (GNSS) is the main positioning system for self-driving vehicles, but it is not accurate enough, so it is integrated with other systems such as light detection and ranging (LiDAR) and inertial navigation systems (INS) to increase the positioning accuracy and availability, especially in urban areas [3].

Placement of antennas on vehicles has large impact on the antenna's performance, so most of the antennas are placed on the vehicle's roof to avoid signal blockage by metal. Roof antennas are usually placed in one cast called a shark-fin due to its shape. Shark-fins have limited size due to the vehicle's aerodynamic design, and recently, many antennas are placed inside these limited size shark-fins, which increase the coupling and shadowing effects between different antennas [4]. One solution to reduce the shadowing
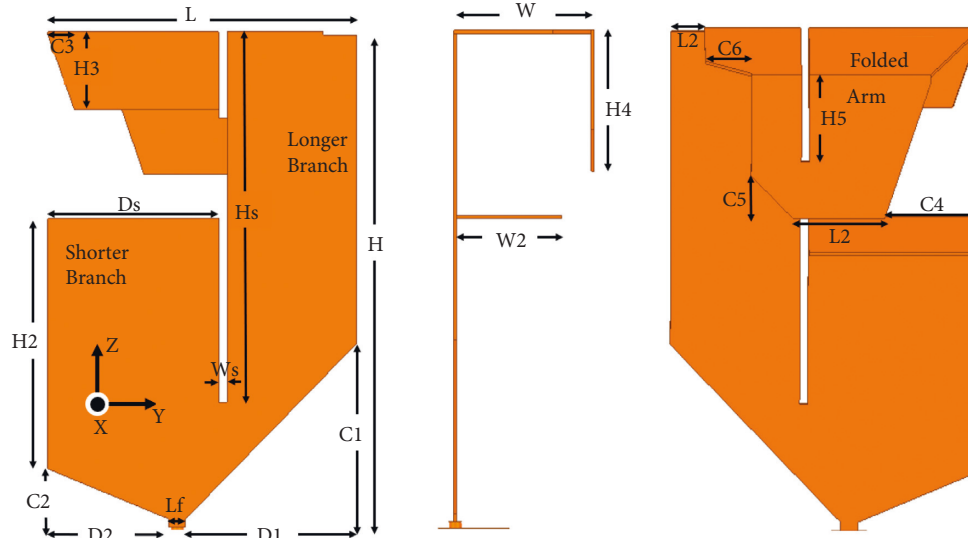
FIGURE 1: Proposed monopole antenna geometry. (a) Front view. (b) Side view. (c) Back view.

TABLE 1: Detailed dimensions of the monopole antenna.

Parameter	Value (mm)	Parameter	Value (mm)	Parameter	Value (mm)
H	58	H4	17	Ds	20.5
L	37	H5	10	C1	22
W	17	Hs	44	C2	7
W2	13	L2	11	C3	3
Ws	1	Lf	2	C4	11.5
H2	30	D1	20.5	C5	5
H3	9.5	D2	14.5	C6	5.5

TABLE 2: Antenna performance requirements.

Application	Frequency (MHz)	VSWR	LAG	Polarization
5G sub-6 GHz and LTE	617–960	3.3	−4 dBi in elevation angles (75°–87°)	Vertical linear polarization
	1710–2690	2.7		
	3300–5000	2.7		
V2X	5850–5925	2	−2 dBi in elevation angles (80°–96°)	Vertical linear polarization
GNSS	1559–1606	2	Active LAG of 20 dBc in elevation angles (0°–50°)	Right-hand circular polarization

and coupling effects on antennas inside a shark-fin is to design antennas that cover multiple bands and applications to reduce the number of antennas as well as reducing the cost [5].

The goal of this paper is to design a compact multiband antenna for the automotive industry that covers 5G sub-6 GHz and LTE cellular frequencies, V2X, and GNSS frequency bands. Most of the automotive cellular antennas found in the literature are for LTE frequency bands starting at 698 MHz to 2690 MHz [6–15]. The most used LTE antenna types are monopoles and planar inverted-F antennas (PIFAs). For the 5G sub-6 GHz, there are fewer antennas in the literature such as the monopole antennas reported in [16–18]. These monopoles antennas cover only 5G sub-6 GHz frequencies and do not cover more frequency bands, and also, they have larger size compared with the proposed antenna. Ultrawide band (UWB) antennas based on

metamaterial and metasurfaces are suitable candidates for the 5G sub-6 GHz [19–22]. A PIFA that covers 5G sub-6 GHz with V2X bands is reported in [23], but it is suitable for certain wide types of shark-fins due to its size. UWB antenna for 5G sub-6 GHz and V2X bands also reported in [24], but it is not suitable to be placed inside a shark-fin.

Usually, vehicles have separate antennas for cellular coverage and navigation due to the polarization difference between these two applications [25, 26]. A few antennas are reported to integrate both GPS and cellular antennas in one antenna element such as the L shaped monopole and the quasi-Yagi antennas, which combine GSM and GPS [27, 28]. These antennas have large size and narrow cellular bandwidth, which makes them not suitable for automotive applications. Stacked antennas with smaller size are also reported for GSM and the Global Positioning System (GPS) but also have narrow cellular bandwidth [29]. From this
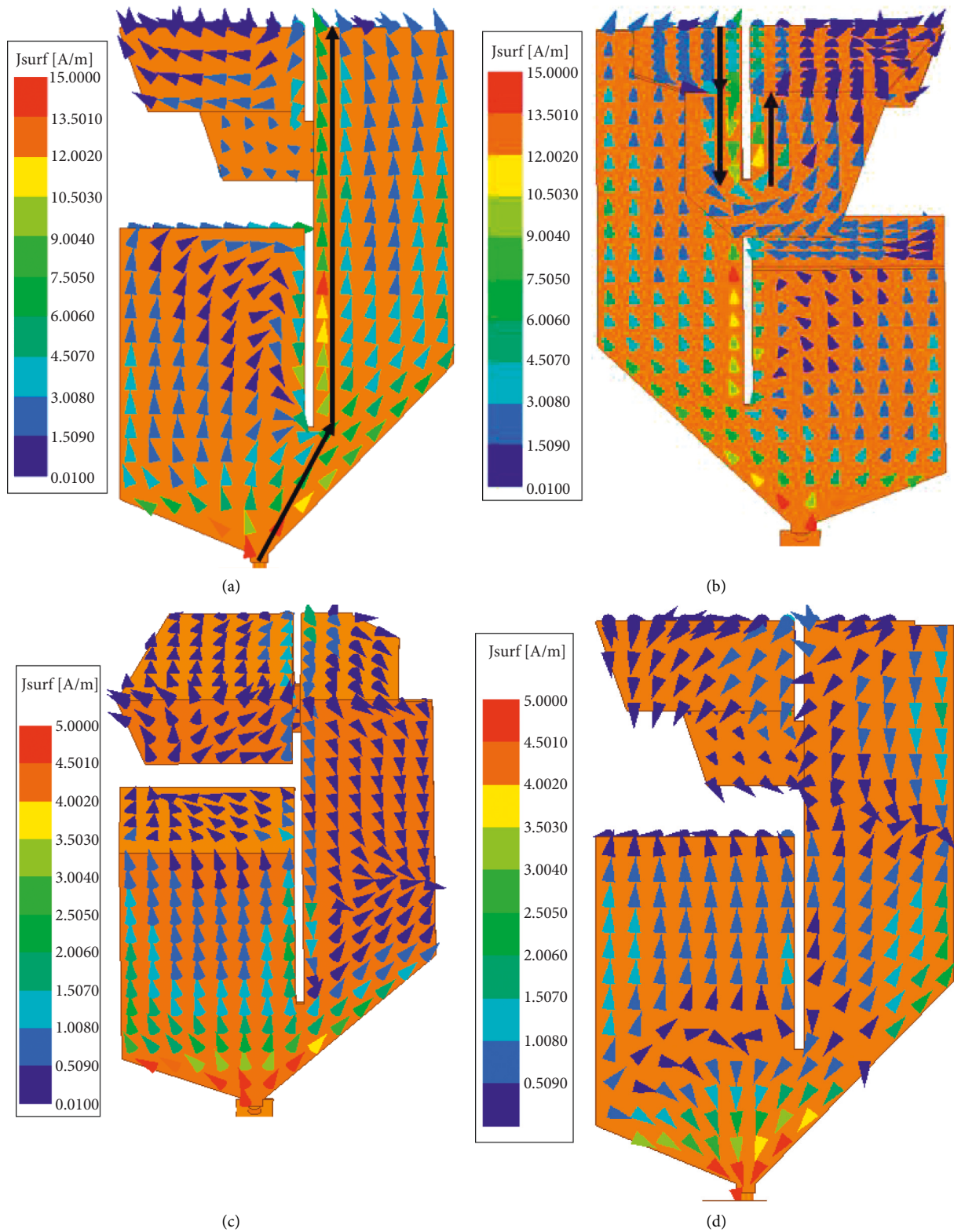
Figure 2: Proposed monopole antenna current distribution. (a) 788 MHz (front view). (b) 788 MHz (back view). (c) 1559 MHz. (d) 5900 MHz.
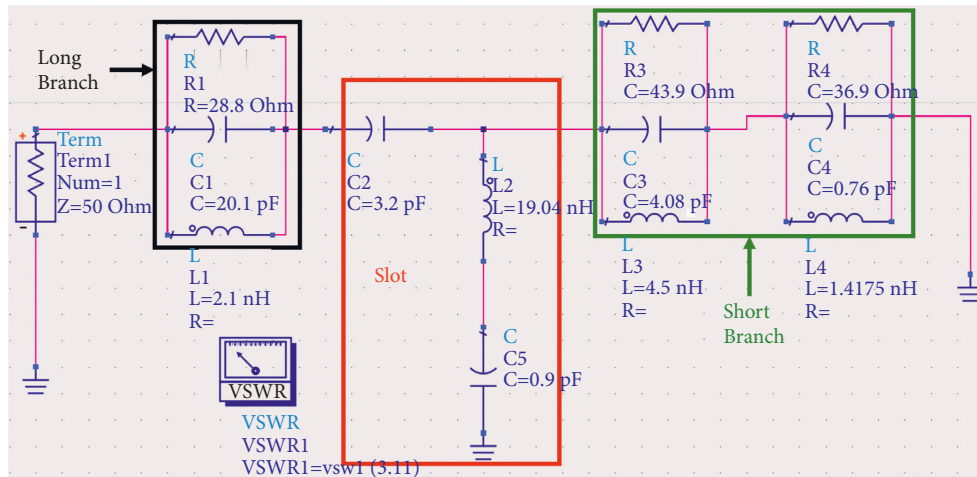
FIGURE 3: Equivalent circuit model of the antenna is reproduced from Alibakhshikenari et al. 2018.
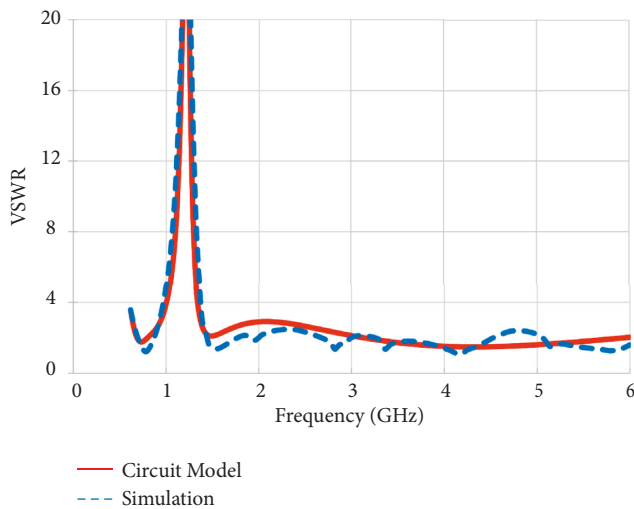

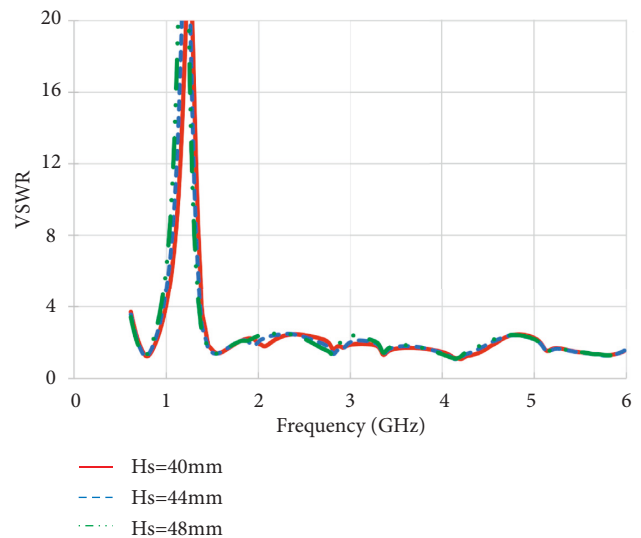FIGURE 4: Simulated and circuit model driven VSWR of the antenna.

FIGURE 6: Effect of the slot length (Hs) on the antenna VSWR.
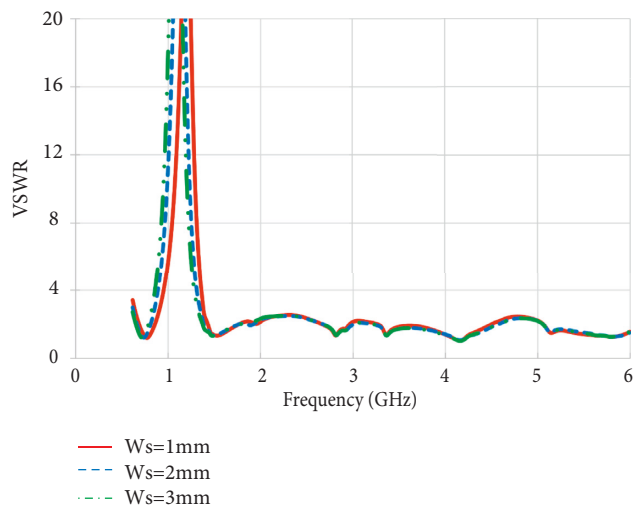

FIGURE 5: Effect of the slot width (Ws) on the antenna VSWR.

literature survey discussion, compact multiband antennas are required for vehicular applications.

In this work, a compact multiband monopole antenna is proposed to cover 5G sub-6 GHz, V2X, and GNSS. The proposed antenna is a three-dimensional metal monopole antenna with two branches to cover this wide bandwidth from 617 MHz to 5925 MHz. Although a monopole antenna is a linear polarized antenna, right-hand circular polarization (RHCP) is measured for GNSS and a GNSS LNA is connected to the antenna to show that the antenna RHCP active gain and radiation pattern shape is suitable for the automotive industry. The antenna design and theory are presented in Section 2, Section 3 discusses the antenna results, and Section 4 concludes this paper.

2. Antenna Design and Theory

The proposed monopole antenna geometry is shown in Figure 1, and Table 1 shows the detailed dimensions of the antenna. The proposed antenna is a folded three-
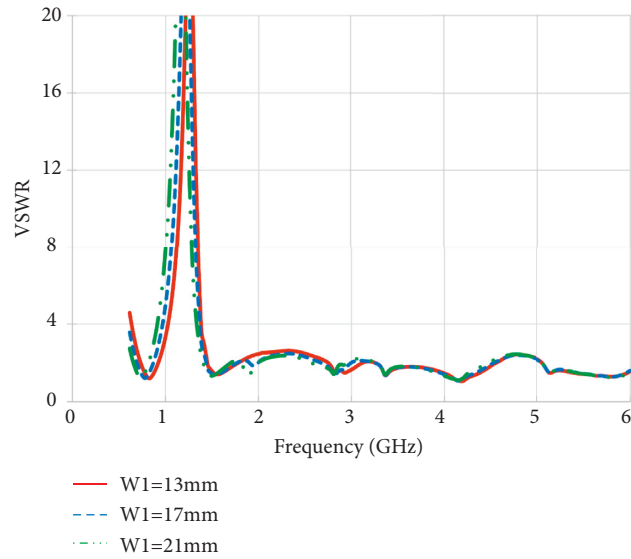
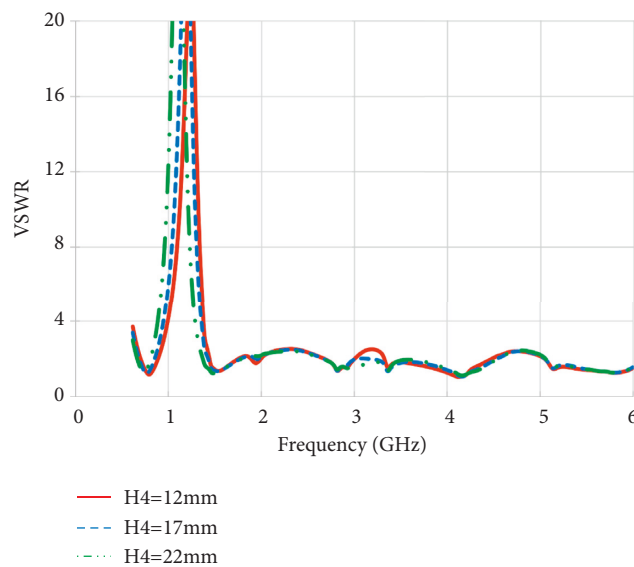FIGURE 7: Effect of the long-branch horizontal folded arm width (W) on the antenna VSWR.

FIGURE 8: Effect of the long-branch vertical folded arm height (H4) on the antenna VSWR.

dimensional monopole antenna with one main slot to divide the antenna into two parts, and these two parts will be called long branch and short branch in the rest of the paper for illustration purposes as shown in Figure 1. The long branch is designed to cover the lower band from 617 to 960 MHz, and this branch is miniaturized by folding the antenna in a horizontal and vertical directions with the slot goes through the two folded parts to lengthen the current path for the antenna to be a quarter wavelength long at 788 MHz, which is the center frequency of the low band. The long-branch folded arm is added to the antenna to reduce the antenna height to fit inside a shark-fin, which has limited height, and the effect of the folded arm will be studied more with the antenna current distribution and parametric sweeps for the

folded arm width (W) and height (H4). The short branch is responsible for the higher band resonance, which is from 1559 to 5925 MHz to cover GNSS, high cellular, and V2X frequency bands. The short branch has a horizontal top loading portion with width W2, this horizontal portion is to make a gap between the short branch and the folded arm of the long branch, and this gap is important for the GNSS signal to not get blocked by the long-branch folded arm, which is also tapered and chamfered for the same purpose. The gap between the short and long branch is optimized to be as large as possible within the antenna dimensions.

The proposed antenna is mounted on an FR4 PCB and connected to a short cable with SMA connector as a feed. The monopole antenna has a compact size (H × L × W) of
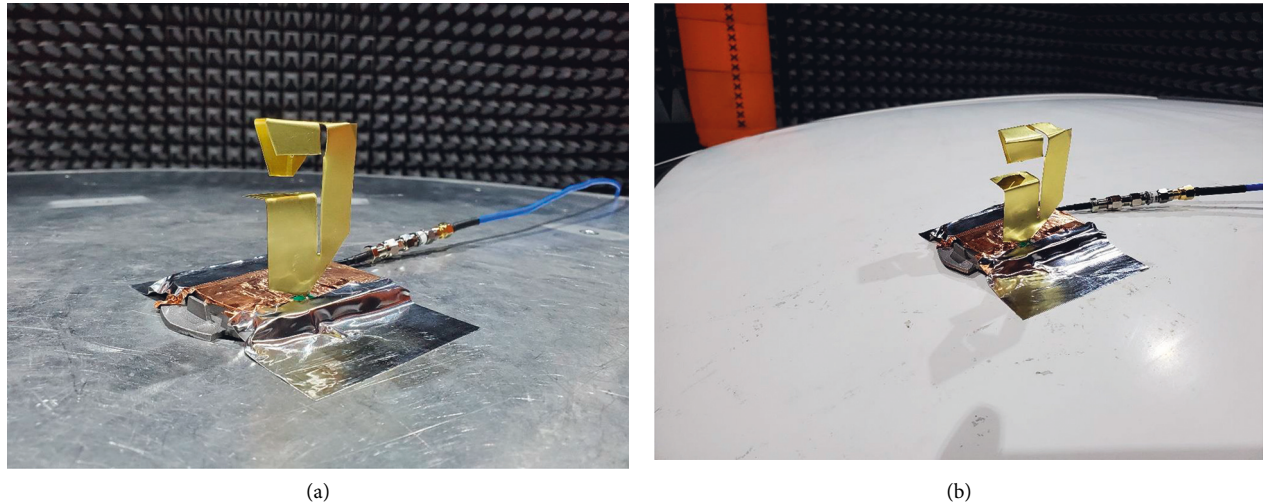
(a)

(b)

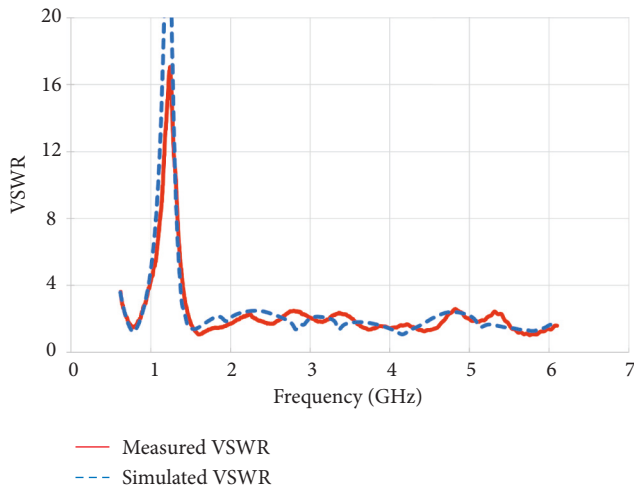FIGURE 9: Fabricated antenna prototype. (a) On ground plane. (b) On vehicle's roof.

FIGURE 10: Proposed antenna simulated and measured VSWR.

$58 \times 37 \times 17$ mm^3. Table 2 shows some general performance requirements that the proposed antenna must meet for 5G, LTE, GNSS, and V2X. The performance requirements are in terms of frequency bands with its corresponding voltage standing wave ratio (VSWR) and the required linear average gain (LAG) in certain elevation angles as well as the polarization. The antenna performance requirements shown in Table 2 are derived from the automotive original equipment manufacturers (OEMs) specifications at the pigtail level [23, 30].

3. Results and Discussions

The proposed monopole antenna was simulated and optimized using ANSYS HFSS. To investigate more on how the antenna covers the required frequency bands, the antenna current distribution is shown in Figure 2 for three different frequencies. For the low-band center frequency (788 MHz), the highest current intensity followed the slot on the long branch as shown by black lines in the front and back views in

Figure 2. The current path length with the highest intensity is measured to be 97 mm, which is very close to the quarter wavelength at 788 MHz (95 mm), and this explains the role of the slot in the proposed antenna miniaturization. For the higher band, which starts at 1559 MHz, the current path length on the short branch can be calculated by $C2+H2+W2$, which is 50 mm, and this is almost equals to the quarter wavelength at 1559 MHz (48 mm). The short branch is responsible for the higher band resonance from 1559 to 5925 MHz.

To develop an equivalent circuit model for the proposed antenna, the antenna simulated VSWR with its geometry will be used. The circuit model is derived from the simulated VSWR using the techniques presented in [31]. Figure 3 shows the proposed monopole antenna equivalent lumped element circuit model, and it consists of three main parts to represent the antenna short branch, long branch, and slot. The slot separates the antenna low band and high band and acts as a band stop filter around 1220 MHz, and this is represented by an LC resonator to ground and a capacitor C2 in series. The antenna long branch, which is responsible for the antenna's low band resonance, is represented by an RLC parallel band pass filter with center frequency of 775 MHz. The short branch is modeled by two parallel RLC band pass filters as the short branch is responsible for the wide high band from 1559 to 5925 MHz, which requires two band pass filters to cover it. The antenna equivalent circuit model is simulated and tuned using Advanced Design System (ADS). Figure 4 shows the VSWR for the circuit model, and for the antenna HFSS simulation, which shows a good agreement, this agreement proves that the circuit model represents the antenna accurately.

Parametric studies on the antenna slot width and length and on the top two-folded long-branch portions were conducted to observe their effects on the antenna resonance. The parametric sweeps were conducted when all the other parameter values are the same as in Table 1. Figure 5 shows the effect of the slot width Ws on the antenna VSWR when Ws changed from 1 to 3 mm. Increasing slot width Ws
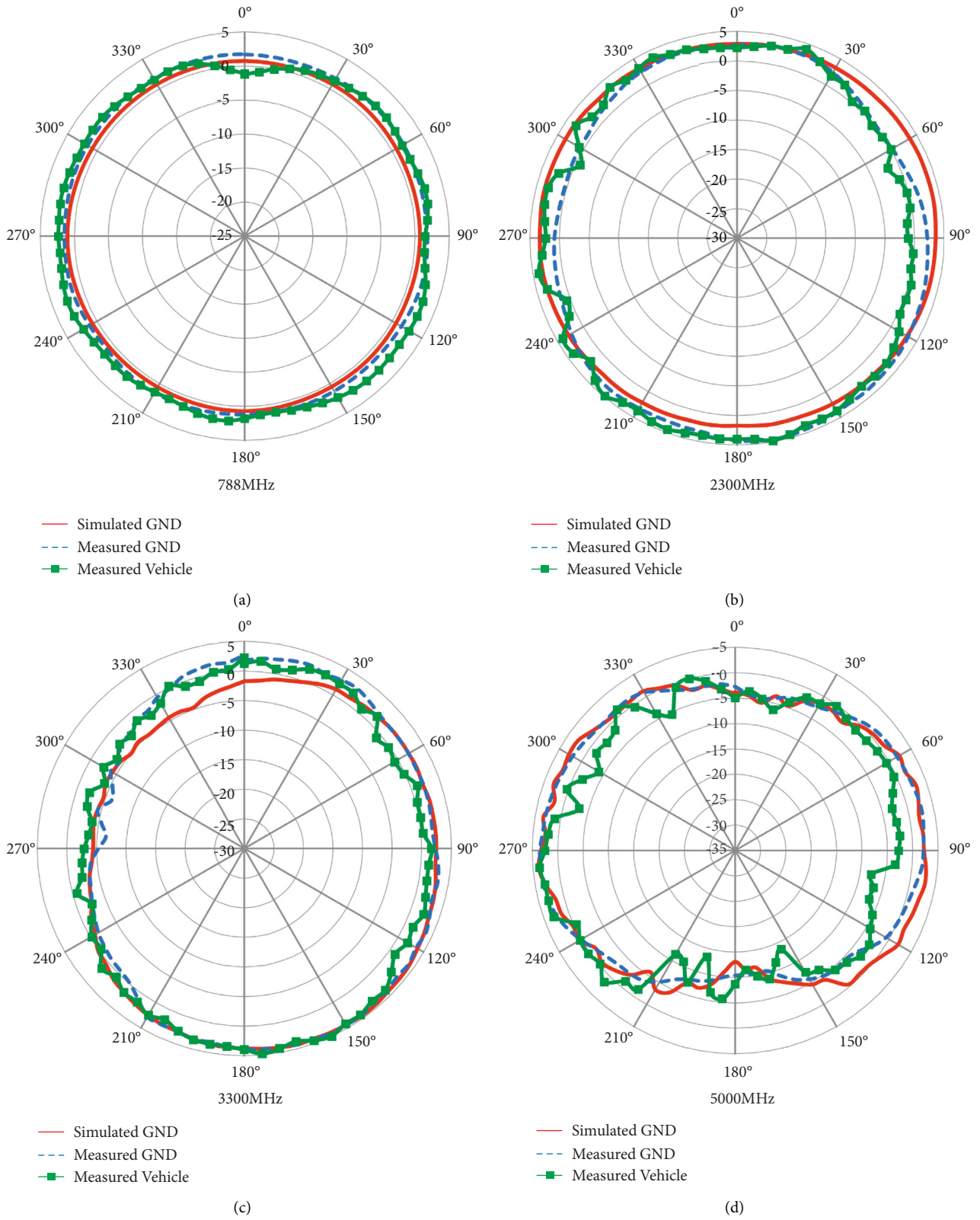
FIGURE 11: Antenna cellular radiation pattern simulated on ground plane and measured on ground plane and a vehicle at 80° elevation angle (0° is the direction of the front of the vehicle). (a) 788 MHz. (b) 2300 MHz. (c) 3300 MHz. (d) 5000 MHz.
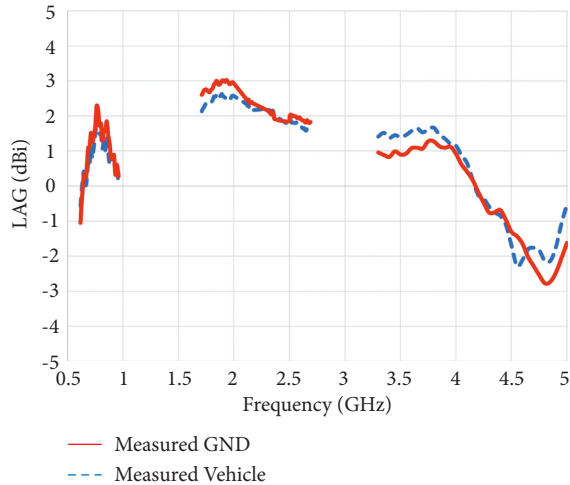
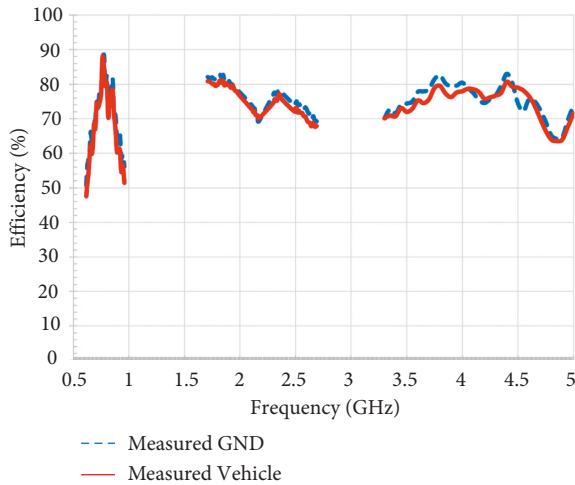Figure 12: 5G and LTE measured LAG on a ground plane and a vehicle.

Figure 13: 5G and LTE measured efficiency on a ground plane and a vehicle.
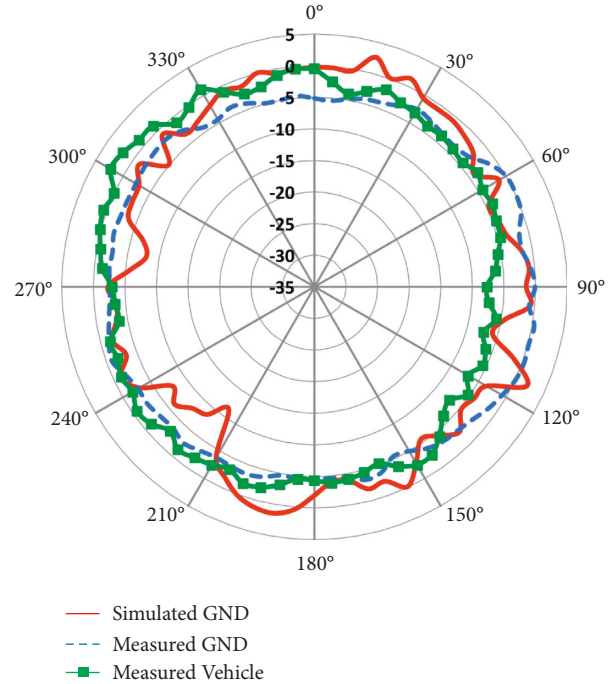

Figure 14: Antenna V2X radiation pattern simulated on ground plane and measured on ground plane and a vehicle at 90° elevation angle at 5900 MHz (0° is the direction of the front of the vehicle).
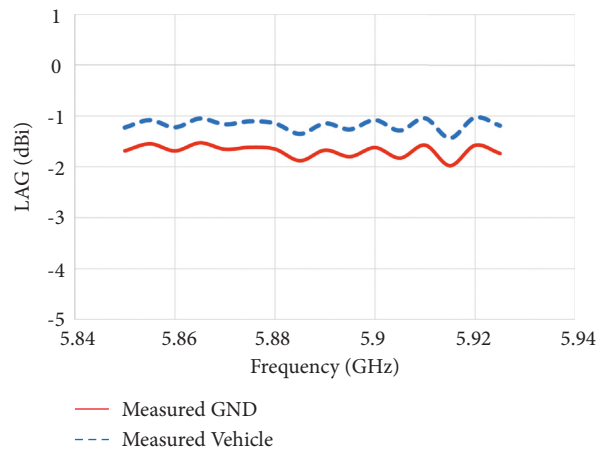
Figure 15: V2X measured LAG on a ground plane and a vehicle roof.

increases the current path, and this results in lowering the resonance frequency for both the low band at 617 MHz and the high band at 1559 MHz when the Ws is 3 mm, and the VSWR at 617 MHz is 2.7 compared with 3.3 when the VSWR is 1 mm, while at 960 MHz, the opposite effect to 617 MHz is observed. At 1559 MHz, increasing Ws shifts the resonance frequency lower, which is the same effect as for 617 MHz. Changing the slot length Hs affects both the low band and the high band due to increasing the current path for both the long and short antenna branches as shown in Figure 6. To conclude on the effect of the slot on the antenna resonance, slot width and length affect antenna low band and high band, increasing the slot width or length shifts the resonance frequency lower at 617 MHz and at 1559 MHz, which is the same effect as increasing inductor L2 or decreasing C5 in the equivalent circuit model shown in Figure 3. On the other hand, decreasing the slot width or length shifts the resonance frequency higher.

Figure 7 shows the effect of the long-branch horizontal folded arm width (W) on the antenna VSWR. Changing W affects the low band at 617 and 960 MHz, increasing W shifts the low-band resonance frequency lower, while decreasing W shifts the low-band resonance frequency higher. Figure 8 shows the effect of the long-branch vertical folded arm height (H4) on the antenna VSWR. Changing H4 mainly affects the low band, increasing H4 shifts the low-band resonance frequency lower and decreasing H4 shifts the low-band resonance frequency higher, which is the same effect as changing W. When increasing H4 to be larger than 20 mm, it starts affecting the higher band at 1559 MHz due to the coupling between long and short branches as the distance

FIGURE 16: V2X measured efficiency on a ground plane and a vehicle roof.

(a)

(b)

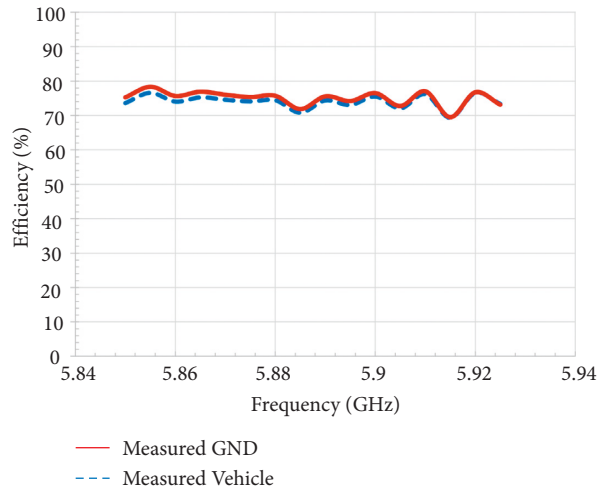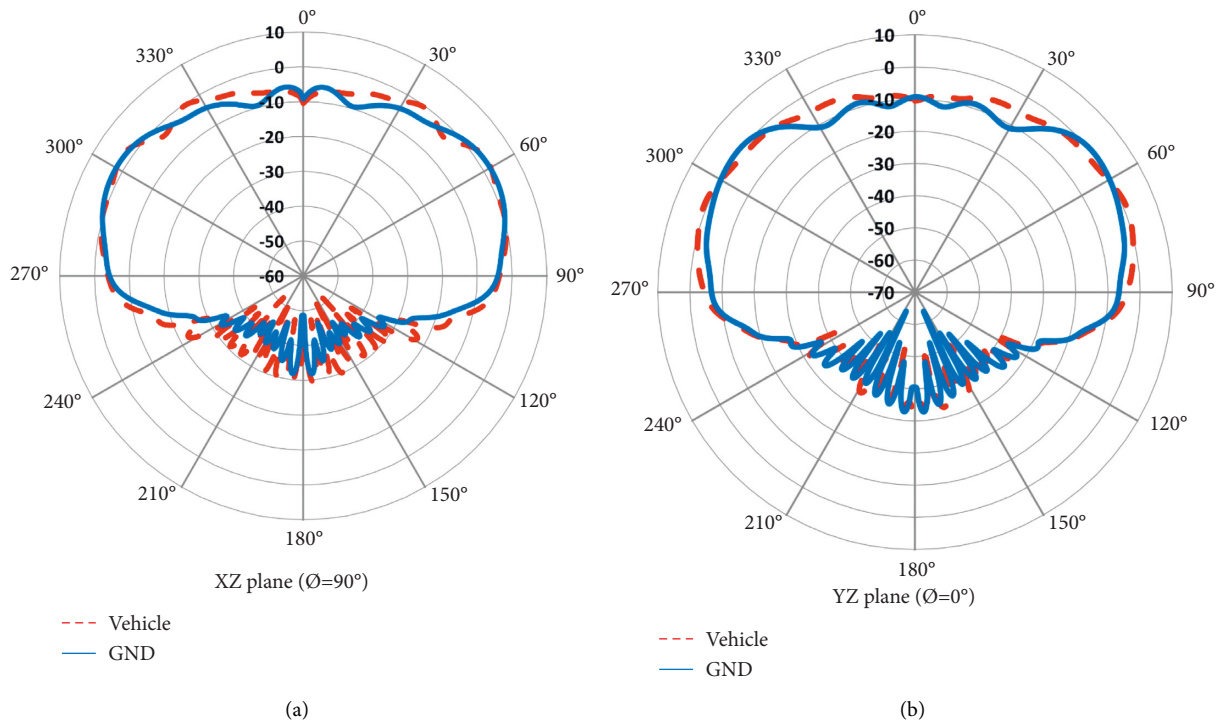FIGURE 17: GNSS passive RHCP gain in the XZ and YZ planes at 1575 MHz measured on ground plane and vehicle. (a) XZ plane (Ø = 90°). (b) YZ plane (Ø = 0°).

between both branches will be small. Changing parameters W or H4 have the same effect of changing inductor L1 and capacitor C1 in the equivalent circuit model.

A prototype for the proposed antenna is fabricated and measured on a one-meter diameter rounded ground plane as well as on vehicle's roof as shown in Figure 9. The antenna VSWR is measured on one-meter ground plane and then compared with the antenna-simulated VSWR as shown in Figure 10. Both simulated and measured VSWR met the antenna VSWR requirements listed in Table 2 for all frequency bands. A good agreement is also achieved between the measured and simulated VSWR as shown in Figure 10.

The fabricated antenna prototype radiation characteristics is measured with a MVG Satimo chamber on a ground plane and then on a vehicle. In the next subsections, the far field measurements are discussed for 5G sub-6 GHz, LTE, V2X, and GNSS.

3.1. 5G Sub-6 GHz and LTE Far-Field Measurements. It is important for the cellular antenna to have an omnidirectional coverage when mounted on a vehicle roof. This omnidirectional radiation is essential in the elevation angles from 75° to 87° (15° to 3° above horizon). Figure 11 shows a
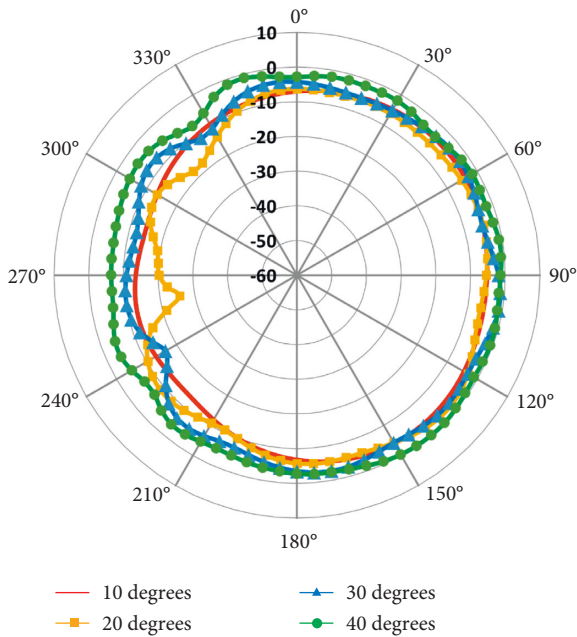
FIGURE 18: Measured GNSS radiation pattern for 4 different elevation angles at 1575 MHz on a ground plane.
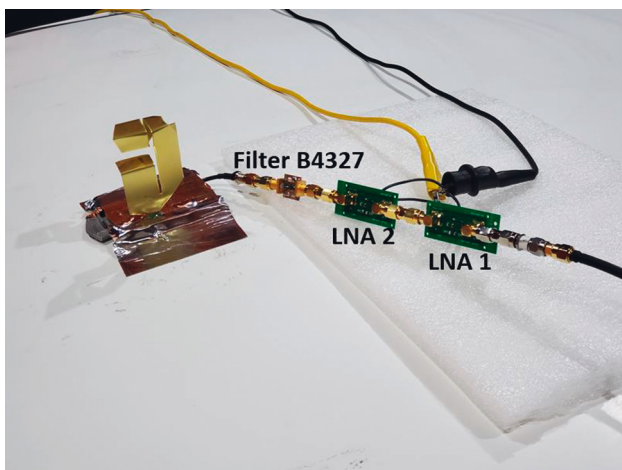

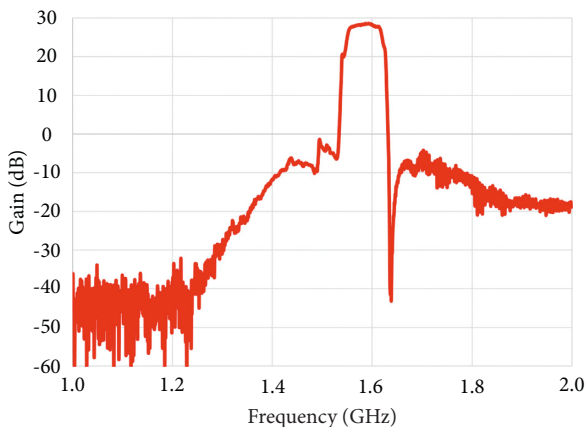FIGURE 19: GNSS active antenna measurements setup on a vehicle.
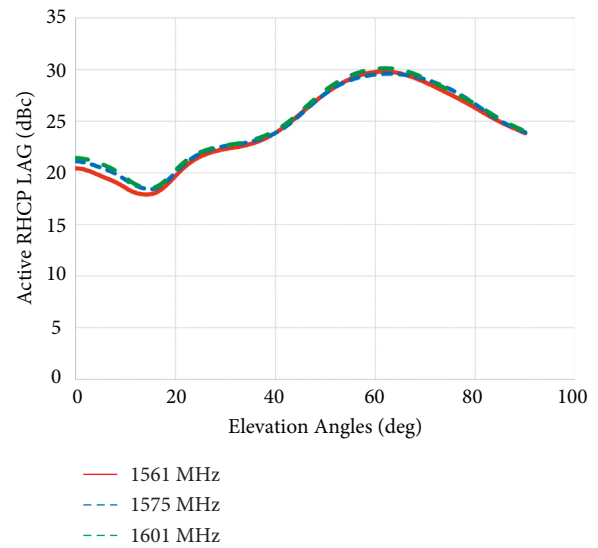

FIGURE 20: Final LNA gain.

FIGURE 21: Measured GNSS active RHCP LAG on a vehicle.

comparison of horizontal cuts of the proposed antenna vertically polarized gain between simulation on a ground plane, measurements on ground plane and on vehicle's roof at 80° elevation angle at frequencies of 788, 2300, 3300, and 5000 MHz. For the low band at 788 MHz, the antenna's radiation pattern is omnidirectional with a good agreement between simulation and measurements. At 2300 and 3300 MHz, the radiation started to be directive, especially in the measurements on both the vehicle and the ground plane. At 5000 MHz, the radiation pattern is more directive to the back and front of the antenna. The vehicle's roof curvature affects the radiation pattern at 5000 MHz as some ripples and reflections started to appear.

In the automotive industry, the antenna gain is expressed in linear average gain (LAG), which can be calculated using the following steps: (1) measure the vertically polarized gain in linear units for 13 elevation angles from 75° to 87° at each of the 360° azimuth angles; (2) calculate the average azimuth gain for each of the 13 elevation angles; and (3) calculate the average gain in linear units from the 13 elevation angles to get one gain value for each frequency and then convert to logarithmic scale (dBi). Figure 12 shows the measured LAG on ground plane and a vehicle. For the low band, the LAG is above -1 dBi for both measurements on the ground plane and vehicle, while the middle band is above 1.5 dBi. After 4 GHz, the LAG is lower due to the reflections that appeared in the 5000 MHz radiation pattern. The proposed antenna LAG meets the LAG requirements listed in Table 2 for the ground plane and vehicle measurements. Figure 13 shows the antenna 5G and LTE measured efficiency on a ground plane and on a vehicle, and the efficiency followed the same curve trend as the LAG curve. For the low band, the efficiency is more than 50% and more than 60% for the high band for both measurement's conditions.

3.2. V2X Far-Field Measurements. Omnidirectional coverage is also important for V2X in elevation angles from 80° to 96°. Figure 14 shows the antenna vertically polarized gain

TABLE 3: Comparison between the proposed monopole antenna and other antennas from the literature.

Reference	Antenna type	Frequency bands (MHz)	Antenna size (mm^3)	Gain/Efficiency	Application
[6]	Printed monopole	698–960 1700–2700	65 × 52 x 1.6	Max gain is more than 1 dBi	Automotive LTE shark-fin application
[13]	T-shaped monopole	698–960 1427–2700	33 × 10 x 55	Max gain is above 2.8 dB/efficiency more than 60%	Vehicular LTE shark-fin application
[30]	Branched monopole	617–960 1710–5000	60 × 39.8 x 15	LAG is above −3 dBi/efficiency more than 50%	Vehicular 5G sub-6 GHz shark-fin application
[16]	Monopole	617–960 1710–5000	60 × 36 x 15	Average gain above −2 dBi/ efficiency more than 45%	Automotive 5G sub-6 GHz shark-fin application
[17]	Folded monopole	700–960 1710–6000	84 × 68 x 0.17	Average gain above 3.9 dBi	Vehicular LTE application
[18]	T-Shaped monopole	720–960 1600–4000	70 × 60 x 1.6	Gain above 1.5 dBi for all bands	Automotive 5G sub-6 GHz application
[23]	PIFA	617–960 1710–6000	55 × 50 x 28	LAG is above −2.5 dBI/efficiency more than 45%	Vehicular 5G sub-6 GHz/V2X shark-fin application
[24]	Nefer ant	698–6000	80 × 60 x 30	Efficiency is above −2 dB Gain is above −3 dB	Vehicular 5G sub-6 GHz/WLAN shark-fin application
This work	Folded monopole	617–960 1559–6000	58 × 37 × 17	LAG is above −3 dBi/efficiency is more than 50%/GNSS coverage	Vehicular 5G sub-6 GHz/GNSS/ V2X shark-fin application

radiation pattern at 5900 MHz and 90° elevation (Horizon) when simulated on ground plane, measured on ground plane, and measured on a vehicle. The measured radiation pattern has a good omnidirectional coverage with maximum gain of 3 dBi and minimum gain of -7 dBi when measured on a vehicle and a maximum gain of 0 dBi and a minimum gain of -5 dBi when measured on a ground plane.

The antenna V2X LAG is calculated following the same steps written in the previous subsection except the V2X elevation angles, which are from 80° to 96°. Figure 15 shows the V2X measured LAG on ground plane and on a vehicle, and the measured LAG on a vehicle is lower than the measured LAG on a ground plane due to the roof curvature. The antenna meets the V2X LAG requirements listed in Table 2.

Figure 16 shows the V2X measured efficiency on a ground plane and a vehicle. The measured efficiency is above 70% for the whole V2X bandwidth.

3.3. GNSS Far-Field Measurements.

Although the monopole antenna is linearly polarized, GNSS measurements were conducted, and the measurements are presented in right-hand circular polarization (RHCP). The targeted GNSS frequency bands are BEIDOU B1 (1559.04–1563.16 MHz), GPS L1 and GALILEO E1 (1574.42–1576.42 MHz), and GLONASS G1 (1597–1606 MHz). Figure 17 shows two vertical cuts (XZ and YZ planes) for the measured GNSS passive RHCP gain at 1575 MHz when mounted on a vehicle and on a ground plane. The two vertical cuts did not show any nulls. The antenna RHCP gain at zenith is -9 dBc and the gain increases until it reaches 0 dBc around 45°. Monopole antennas have low gain at zenith, and when converting the linear polarized gain into RHCP gain, another 3 dBi is subtracted and this is the reason its RHCP gain at zenith is −9 dBc.

To check the antenna GNSS coverage, horizontal cuts for four different elevation angles (10°, 20°, 30°, and 40°) measured on ground plane at 1575 MHz are shown in Figure 18. The proposed antenna shows good radiation pattern without major nulls in angles of interest; however, the antenna has better coverage to the front of the antenna (azimuth angles from 0° to 180°) than to the back of it (azimuth angles from 180° to 360°).

To measure the antenna active performance, low noise amplifier (LNA) is constructed using two LNA stages of signal processing LNA-00120 connected to a Qualcomm GNSS Saw Filter (B4327) to provide the required isolation as shown in Figure 19. Figure 20 shows the S21 of the constructed LNA, which has a gain of 28 dB in the GNSS frequency band and a good isolation in the other bands. The LNA has the same gain as an automotive grade GNSS LNA gain.

Figure 21 shows the measured GNSS active RHCP LAG on a vehicle at the center frequencies of BEIDOU, GPS, and GLONASS, which are 1561, 1575, and 1601 MHz, respectively. The LAG is calculated for each elevation angle by averaging azimuth angles. The active RHCP LAG is more than 20 dBc for most of the elevation angles considering using an LNA with normal gain value for automotive industry. This shows that the proposed antenna can receive GNSS signals with acceptable gain despite the antenna's dominant linear polarization. Adding GNSS to the antenna makes the antenna design challenging as the antenna long branch can block the GNSS signal if not designed carefully, and this is the reason for the chamfering and tapering in the upper folded parts of the antenna long branch.

Table 3 shows a comparison between the proposed monopole antenna and other automotive antennas with wide bandwidth found in the literature. Most of the listed antennas covers the cellular bands. Two antennas cover cellular and V2X frequency bands [23, 24] with larger size than the proposed antenna, which covers the GNSS higher band too.

4. Conclusions

A compact monopole antenna is designed to cover multi-frequency bands for the automotive industry. The multiband

antenna covers 5G sub-6 GHz, LTE, GNSS higher frequency band, and V2X. The proposed antenna is a three-dimensional monopole antenna with two branches to cover the enlarged bandwidth required which starts from 617 MHz to 6 GHz. The antenna is simulated and optimized, and then, a prototype is fabricated and measured on one-meter ground plane and on a vehicle roof. The antenna measurements are expressed in terms of VSWR, radiation pattern, LAG, and efficiency in which the presented antenna showed good results that met the performance requirements. The proposed antenna has measured efficiency of 50–90% in the operating frequency and LAG of −2.2 to 3 dBi across the entire frequency band. A good agreement is achieved between the simulated and measured results. The antenna is optimized to enhance the GNSS performance, and the active RHCP LAG is measured, which was more than 20 dBi in most of elevation angles using normal 28-dB automotive GNSS LNA.

Data Availability

The data used to support the findings of this paper are included within the article.

Conflicts of Interest

The authors declared that they have no conflicts of interest regarding the publication of this paper.

Supplementary Materials

The raw data of the figures of the article are added as supplemental materials. (*Supplementary Materials*)

References

[1] M. Alibakhshikenari, B. S. Virdee, C. H. See et al., "Dual-polarized highly folded bowtie antenna with slotted self-grounded structure for sub-6 GHz 5G applications," *IEEE Transactions on Antennas and Propagation*, vol. 70, no. 4, pp. 3028–3033, 2021.

[2] S. Gyawali, S. Xu, Y. Qian, and R. Q. Hu, "Challenges and solutions for cellular based V2X communications," *IEEE Communications Surveys & Tutorials*, vol. 23, no. 1, pp. 222–255, 2021.

[3] W. W. Wen, G. Zhang, and L.-T. Hsu, "GNSS NLOS exclusion based on dynamic object detection using LiDAR point cloud," *IEEE Transactions on Intelligent Transportation Systems*, vol. 22, no. 2, pp. 853–862, Feb. 2021.

[4] M. Alibakhshikenari, E. Limiti, M. Naser-Moghadasi, B. S. Virdee, and R. Sadeghzadeh, "A new wideband planar antenna with band-notch functionality at GPS, Bluetooth and WiFi bands for integration in portable wireless systems," *AEU - International Journal of Electronics and Communications*, vol. 72, pp. 79–85, 2017.

[5] G. Artner, W. Kotterman, G. Del Galdo, and M. A. Hein, "Automotive antenna roof for cooperative connected driving," *IEEE Access*, vol. 7, pp. 20083–20090, 2019.

[6] D. Preradov and D. N. Aloi, "Cross polarized 2x2 LTE MIMO system for automotive shark fin application," *Applied Computational Electromagnetics Society*, vol. 35, no. 10, pp. 1207–1216, 2020.

[7] Y. Dong, J. Choi, and T. Itoh, "Vivaldi antenna with pattern diversity for 0.7 to 2.7 GHz cellular band Applications," *IEEE Antennas and Wireless Propagation Letters*, vol. 17, no. 2, pp. 247–250, Feb. 2018.

[8] S. Arianos, G. Dassano, F. Vipiana, and M. Orefice, "Design of multi-frequency compact antennas for automotive communications," *IEEE Transactions on Antennas and Propagation*, vol. 60, no. 12, pp. 5604–5612, 2012.

[9] A. Michel, P. Nepa, M. Gallo, I. Moro, A. P. Filisan, and D. Zamberlan, "Printed wideband Antenna for LTE-band Automotive applications," *IEEE Antennas and Wireless Propagation Letters*, vol. 16, pp. 1245–1248, 2017.

[10] Y. Liu, Z. Ai, G. Liu, and Y. Jia, "An integrated shark-fin antenna for MIMO-LTE, FM, and GPS applications," *IEEE Antennas and Wireless Propagation Letters*, vol. 18, no. 8, pp. 1666–1670, Aug, 2019.

[11] V. Franchina, A. Michel, P. Nepa, M. Gallo, and R. Parolari, "A compact 3D antenna for automotive LTE MIMO applications," in *Proceedings of the 2017 IEEE-APS Topical Conference on Antennas and Propagation in Wireless Communications*, pp. 326–329, APWC, Verona Italy, September 2017.

[12] A. Friedrich, B. Geck, O. Klemp, and H. Kellermann, "On the design of a 3D LTE antenna for automotive applications based on MID technology," in *Proceedings of the 2013 European Microwave Conference*, pp. 640–643, Nuremberg Germany, October 2013.

[13] I. Goncharova and S. Lindenmeier, "A high efficient automotive roof-antenna concept for LTE, DAB-L, GNSS and SDARS with low mutual coupling," in *Proceedings of the 2015 9th European Conference on Antennas and Propagation*, pp. 1–5, EuCAP, Lisbon, Portugal, April 2015.

[14] I. Goncharova and S. Lindenmeier, "A high-efficient 3-D Nefer-antenna for LTE communication on a car," in *Proceedings of the 8th European Conference on Antennas and Propagation*, pp. 3273–3277, EuCAP, The Hague, Netherlands, April 2014.

[15] D. V. Navarro-Méndez, L. F. Carrera-Suarez, E. Antonino-Daviu et al., "Compact wideband vivaldi monopole for LTE mobile communications," *IEEE Antennas and Wireless Propagation Letters*, vol. 14, pp. 1068–1071, 2015.

[16] A. M. Yacoub, M. O. Khalifa, and D. N. Aloi, "Design of multi-wideband Automotive cell antenna for LTE and 5G applications," *2021 15th European Conference on Antennas and Propagation*, EuCAP, 2021.

[17] B. Sanz-Izquierdo, S. Jun, J. Heirons, and N. Acharya, "Inkjet printed and folded LTE antenna for vehicular application," in *Proceedings of the 2016 46th European Microwave Conference (EuMC)*, pp. 88–91, London, UK, October 2016.

[18] Y. Cheng and J. Lu, "Can wang, "design of a multiple band vehicle-mounted antenna," *International Journal of Antennas and Propagation*, vol. 2019, Article ID 6098014, 11 pages, 2019.

[19] R. A. Sadeghzadeh, M. Alibakhshi-Kenari, and M. Naser-Moghadasi, "UWB antenna based on SCRLH-TLs for portable wireless devices," *Microwave and Optical Technology Letters*, vol. 58, no. 1, pp. 69–71, 2016.

[20] M. Alibakhshi-Kenari, M. Naser-Moghadasi, R. Ali Sadeghzadeh, and B. Singh Virdee, "Metamaterial-based antennas for integration in UWB transceivers and portable microwave handsets," *International Journal of RF and Microwave Computer-Aided Engineering*, vol. 26, no. 1, pp. 88–96, 2016.

[21] M. Alibakhshi-Kenari, M. Naser-Moghadasi, R. Ali Sadeghzadeh, B. Singh Virdee, and E. Limiti, "New compact antenna based on simplified CRLH-TL for UWB wireless

communication systems," *International Journal of RF and Microwave Computer-Aided Engineering*, vol. 26, no. 3, pp. 217–225, 2016.

[22] M. Alibakhshikenari, B. S. Virdee, A. Ali, and E. Limiti, "Extended aperture miniature antenna based on CRLH metamaterials for wireless communication systems operating over UHF to C-band," *Radio Science*, vol. 53, no. 2, pp. 154–165, Feb. 2018.

[23] A. Yacoub, M. Khalifa, and D. N. Aloi, "Wide bandwidth low profile PIFA antenna for vehicular sub-6 GHz 5G and V2X wireless systems," *Progress In Electromagnetics Research C*, vol. 109, pp. 257–273, 2021.

[24] S. Hastürkoğlu and S. Lindenmeier, "A wideband automotive antenna for actual and future mobile communication 5G/LTE/WLAN with low profile," in *Proceedings of the 2017 11th European Conference on Antennas and Propagation*, pp. 602–605, EUCAP, Paris France, March 2017.

[25] J. D. Doherty, I. Shoaib, X. Chen, and C. Parini, "Study and design of an integrated GPS and cellular antenna," in *Proceedings of the 2013 Loughborough Antennas & Propagation Conference*, pp. 587–590, LAPC, Loughborough, UK, November 2013.

[26] O.-Y. Kwon, R. Song, and B.-S. Kim, "A fully integrated shark-fin antenna for MIMO-LTE, GPS, WLAN, and WAVE applications," *IEEE Antennas and Wireless Propagation Letters*, vol. 17, no. 4, pp. 600–603, April 2018.

[27] P. Mousavi, "Multiband multipolarization integrated monopole slots antenna for vehicular telematics applications," *IEEE Transactions on Antennas and Propagation*, vol. 59, no. 8, pp. 3123–3127, Aug, 2011.

[28] S. J. Wu, C. H. Kang, K. H. Chen, and J. H. Tarng, "A multiband quasi-yagi type Antenna," *IEEE Transactions on Antennas and Propagation*, vol. 58, no. 2, pp. 593–596, Feb. 2010.

[29] Y. Wang, Y. Li, and Q. Zhu, "A compact tri-band antenna for GPS and GSM applications," in *Proceedings of the 2017 Sixth Asia-Pacific Conference on Antennas and Propagation*, pp. 1–3, APCAP, Xi'an, China, October 2017.

[30] M. O. Khalifa, A. M. Yacoub, and D. N. Aloi, "A multi-wideband compact antenna design for vehicular sub-6 GHz 5G wireless systems," *IEEE Transactions on Antennas and Propagation*, vol. 69, no. 12, pp. 8136–8142, Dec, 2021.

[31] K. Sayidmarie and L. Yahya, "Modeling of dual-band crescent-shape monopole antenna for WLAN applications," *International Journal of Electromagnetics and Applications*, vol. 4, pp. 31–39, 2014.